

Controversial electronic structures and energies of Fe², Fe²⁺, and Fe²⁻ resolved by RASPT2 calculations

Chad E. Hoyer, Giovanni Li Manni, Donald G. Truhlar, and Laura Gagliardi

Citation: *The Journal of Chemical Physics* **141**, 204309 (2014); doi: 10.1063/1.4901718

View online: <http://dx.doi.org/10.1063/1.4901718>

View Table of Contents: <http://scitation.aip.org/content/aip/journal/jcp/141/20?ver=pdfcov>

Published by the [AIP Publishing](#)

Articles you may be interested in

Calculation of the structure, potential energy surface, vibrational dynamics, and electric dipole properties for the Xe:HI van der Waals complex

J. Chem. Phys. **134**, 174302 (2011); 10.1063/1.3583817

The electronic structure of the triiodide ion from relativistic correlated calculations: A comparison of different methodologies

J. Chem. Phys. **133**, 064305 (2010); 10.1063/1.3474571

An accurate first principles study of the geometric and electronic structure of B₂, B₂⁻, B₃, B₃⁻, and B₃H: Ground and excited states

J. Chem. Phys. **132**, 164307 (2010); 10.1063/1.3389133

A theoretical and computational study of the anion, neutral, and cation Cu (H₂O) complexes

J. Chem. Phys. **121**, 5688 (2004); 10.1063/1.1782191

Geometries and spectroscopic properties of silicon clusters (Si₅, Si₅⁺, Si₅⁻, Si₆, Si₆⁺, and Si₆⁻)

J. Chem. Phys. **116**, 3690 (2002); 10.1063/1.1446027



Controversial electronic structures and energies of Fe_2 , Fe_2^+ , and Fe_2^- resolved by RASPT2 calculations

Chad E. Hoyer, Giovanni Li Manni, Donald G. Truhlar,^{a)} and Laura Gagliardi^{a)}

Department of Chemistry, Chemical Theory Center, and Supercomputing Institute, University of Minnesota, 207 Pleasant St. SE, Minneapolis, Minnesota 55455-0431, USA

(Received 12 July 2014; accepted 3 November 2014; published online 26 November 2014)

The diatomic molecule Fe_2 was investigated using restricted active space second-order perturbation theory (RASPT2). This molecule is very challenging to study computationally because predictions about the ground state and excited states depend sensitively on the choice of the quantum chemical method. For Fe_2 we show that one needs to go beyond a full-valence active space in order to achieve even qualitative agreement with experiment for the dissociation energy, and we also obtain a smooth ground-state potential curve. In addition we report the first multireference study of Fe_2^+ , for which we predict an $^8\Sigma_u^-$ ground state, which was not predicted by previous computational studies. By using an active space large enough to remove the most serious deficiencies of previous theoretical work and by explicitly investigating the interpretations of previous experimental results, this study elucidates previous difficulties and provides – for the first time – a qualitatively correct treatment of Fe_2 , Fe_2^+ , and Fe_2^- . Moreover, this study represents a record in terms of the number of active electrons and active orbitals in the active space, namely 16 electrons in 28 orbitals. Conventional CASPT2 calculations can be performed with at most 16 electrons in 16 orbitals. We were able to overcome this limit by using the RASPT2 formalism. © 2014 AIP Publishing LLC. [<http://dx.doi.org/10.1063/1.4901718>]

I. INTRODUCTION

Iron clusters exhibit interesting trends in reactivity and ionization potentials (IPs) over a range of cluster sizes.^{1–7} There have been several quantum chemical studies of iron clusters based on Kohn-Sham density functional theory;^{8–11} however, important questions remain, even for the smallest ones, Fe_2 , Fe_2^+ , and Fe_2^- . For example, the natures of the ground states of Fe_2 and Fe_2^+ are unresolved in previous work. This indicates that even the smallest clusters are still very challenging and they are the objects of the present study. For a complete understanding of these issues, we first discuss the experimental and theoretical background.

A. Previous experimental work

A ground-state vibrational frequency (ω_e) of 299.6 cm^{-1} was measured for Fe_2 in both solid Ar and solid Kr matrices at 11 K with resonance Raman spectroscopy.¹² The authors tested for the presence of Fe_2 by measuring the absorbance of their sample and comparing it with that previously reported.¹³ The most accurate ground-state bond length (R_e), $2.02 \pm 0.02\text{ \AA}$, was obtained from an extended x-ray absorption fine structure (EXAFS) study performed on Fe_2 isolated in solid neon at 4 K.¹⁴ However, recent computational^{11,15} and experimental^{16,17} studies disagree on the symmetry of the ground state of Fe_2 .

In 1984, Baumann *et al.* attempted to measure an electron paramagnetic resonance (EPR) spectrum of Fe_2 in an Ar

and a Kr matrix at 4 K;¹⁷ no transition was observed. Because the experimental conditions were similar to the EXAFS study and they observed little zero-field splitting (ZFS) in other transition-metal complexes,¹⁸ they concluded that Fe_2 most likely has an orbitally degenerate ground state. (An orbitally degenerate state is a molecular electronic state with, in the absence of spin-orbit coupling, two or more degenerate components due to orbital angular momentum. For a linear molecule this corresponds to a nonzero value for the orbital angular momentum projection quantum number Λ , as in a Π state). In the EPR study, the observed transitions between the M_s components obey the following relation: $h\nu \propto \mathbf{D} \pm g\beta B$, where h is Planck's constant, ν is frequency, \mathbf{D} is the ZFS parameter, g is the g-tensor, β is the Bohr magneton, and B is the magnitude of the magnetic field.¹⁹ For a linear molecule in a solid matrix (as in the case of Fe_2) with an orbitally degenerate ground state, the g-tensor may be very anisotropic, and one of the components is zero (implying that an infinite magnetic field would be needed to induce a transition).²⁰ No clear transition occurs since the random orientations of the molecules in the matrix cause weak absorptions to occur over an extended range of magnetic field.²⁰ Now, going back to the effects of ZFS on the EPR spectrum, iron dimer would need a ZFS parameter D (D is a scalar due to the symmetry of the problem) around 8 cm^{-1} or greater for it not to be observed if it does not have an orbitally degenerate ground state.¹⁷

In 1986, the photoelectron spectrum of Fe_2 was measured in the gas phase with negative ion photoelectron (PE) spectroscopy.^{16,21} From the spectrum, the ground-state configurations for Fe_2^- and Fe_2 were assigned as $4s^43d^{13}$ and $4s^33d^{13}$ respectively (the configuration specification convention used in the present article labels configurations with

^{a)}Authors to whom correspondence should be addressed. Electronic addresses: truhlar@umn.edu and gagliardi@umn.edu.

respect to the separated atoms: $\text{Fe}^-(4s^23d^7) + \text{Fe}(4s^23d^6)$ and $\text{Fe}(4s^23d^6) + \text{Fe}^*(4s^13d^7)$). A 0.90 eV electron affinity (EA) was also measured.¹⁶ It was concluded that the state observed for Fe_2 was the ground state because of the good agreement in vibrational frequency with that of the resonance Raman study.

The ionization potential of Fe_2 was measured by Rohlfing *et al.* by employing photoionization spectroscopy in the gas phase.⁶ Whether the ground state of Fe_2^+ can be formed by one-electron detachment from Fe_2 has yet to be investigated.

The dissociation energy (D_0) of Fe_2 was measured indirectly by first measuring the dissociation energy of Fe_2^+ through collision-induced dissociation (CID) methods.²² In addition to the IPs of Fe and Fe_2 , the D_0 of Fe_2^+ was used to compute the D_0 for Fe_2 according to the following equation:

$$D_0(\text{Fe}_2) = D_0(\text{Fe}_2^+) - IP(\text{Fe}) + IP(\text{Fe}_2). \quad (1)$$

Analogously to Eq. (1), the D_0 of Fe_2^- was also computed with experimental quantities.

B. Previous theoretical work

In 2002 and 2003, two quantum chemical studies to characterize the states observed in the negative ion PE study were reported.^{23,24} Both used a complete-active space self-consistent-field (CASSCF)²⁵ reference wave function with an active space of 16 electrons in 12 orbitals, denoted CAS(16,12). Bauschlicher and Ricca²³ used both calculations employing multireference configuration interaction plus a Davidson correction (MRCI+Q^D)^{26,27} and calculations employing CAS second-order perturbation theory (CASPT2).^{28,29} By a CASPT2(16,12) calculation they predicted that the $^9\Sigma_g^-$ state with a $4s^33d^{13}$ configuration is the lowest-energy state of Fe_2 . However, their results with CASPT2(16,15) in which they added correlating $3d$ orbitals to the CAS(16,12) active space indicated that the ground state is a $^7\Delta_u$ state with a $4s^23d^{14}$ configuration (i.e., that is corresponds to separated atoms with configurations $\text{Fe}^*(4s^13d^7) + \text{Fe}^*(4s^13d^7)$, where * denotes an excited state). The conclusion was based on the lowering of the computed $^9\Sigma_g^- - ^7\Delta_u$ splitting from 0.84 eV with CAS(16,12) to 0.19 eV with CAS(16,15), and it was hypothesized that larger active spaces would decrease the splitting further until negative values are reached. For Fe_2^- a CASPT2 calculation with a (17,12) active space predicted that an $^8\Sigma_u^-$ state with a $4s^43d^{13}$ configuration is the ground state. The authors said that there was good agreement between their calculations and EPR result for Fe_2 because an orbitally degenerate state was predicted. They provided a possible explanation of the negative ion PE experiment, namely that although the $^7\Delta_u$ is the ground state, it was not observed because it cannot be formed from a one-electron detachment from the $^8\Sigma_u^-$ state of Fe_2^- , and electron detachment from the $^8\Sigma_u^-$ electronic state of Fe_2^- was inferred to lead to the $^9\Sigma_g^-$ state of Fe_2 .

A second computational characterization of Fe_2 and Fe_2^- was performed by Hübner and Sauer.²⁴ They also used a CASSCF(16,12) wave function as a reference and they re-

ported a multireference configuration interaction (MRCI) calculation with a Pople size-consistency correction, Q^P.³⁰ The $^8\Sigma_u^-$ and $^9\Sigma_g^-$ states were predicted to be the ground states of Fe_2^- and Fe_2 , respectively. This picture agrees well with the negative ion PE experiment but disagrees with the EPR result because Σ states are not orbitally degenerate.

Inconsistencies are still present in very recent computational studies; we give two examples. In 2011, the calculations of Angeli and Cimraglia predicted a $^9\Sigma_g^-$ ground state for Fe_2 .¹⁵ They used a CASSCF reference wave function with a (16,12) active space in a calculation by N -electron valence state perturbation theory up to second order (NEVPT2) and third order (NEVPT3).³¹ However, the authors performed tests on a single Fe atom from which they concluded that the CAS(16,12) active space for Fe_2 is too small. An indication of the difficulty of treating all relevant configurations adequately is that their $^7\Delta_u$ potential energy curves showed large discontinuities at all levels of theory that they employed.

In 2012, Cervantes-Salguero and Seminario predicted a $^7\Delta_u$ ground state for Fe_2 , using the OPBE^{32,33} exchange-correlation functional.¹¹

Given the inconsistencies among various computational results on the Fe_2 , Fe_2^+ , and Fe_2^- systems we decided to undertake a computational study of these systems with multireference methods based on restricted active space self-consistent field wave functions. We show results obtained employing wave functions generated by a larger numbers of active electrons and orbitals (16 electrons in 28 orbitals) than have been treated previously. We discuss why such a large active space is needed to obtain quantitatively correct results. Our computational study represents a record in terms of the size of the active space employed. Conventional CASPT2 calculations can be performed with at most 16 electrons in 16 orbitals. We were able to go beyond this limit by using the RASSCF and RASPT2 formalism.

II. COMPUTATIONAL METHODS

Because CAS calculations with a large enough active space to yield a realistic potential energy curve would be too large to be practical, we employ the restricted active space self-consistent field (RASSCF)³⁴ method followed by second-order perturbation theory (RASPT2).³⁵ All RASSCF and RASPT2 calculations were performed with the MOLCAS 7.8 software package.³⁶ A basis set of the atomic-natural-orbital type³⁷ of quadruple- ζ plus polarization quality (ANO-RCC-VQZP) [7s6p4d3f2g1h] was used. Scalar relativistic effects were included by using the second-order Douglas-Kroll-Hess Hamiltonian.³⁸ All RASSCF calculations used a level shift of 0.5 hartree.³⁹ All RASPT2 calculations utilized an imaginary shift of 0.2 hartree⁴⁰ to eliminate intruder states. A modified zeroth-order Hamiltonian was used that incorporated an ionization potential–electron affinity (IPEA) shift of 0.25 hartree.⁴¹ Except where noted otherwise, all calculations were performed by imposing the symmetry constraints of the D_{2h} point group.

The active spaces used here are denoted RAS($n,N;p,P$), which denotes a distribution of n electrons in $N + P$ orbitals such that all possible CSFs involving various

occupancies of N orbitals (called the RAS2 orbitals) are included plus additional CSFs with up to p electrons in P additional orbitals (called the RAS3 orbitals) and the rest in the original N orbitals. In this notation a CAS active space would be CAS($n,N;0,0$). For our calculations on the diatomic systems, we use RAS($n,12;2,16$) where $n = 15, 16$, and 17 for Fe_2^+ , Fe_2 , and Fe_2^- , respectively. In the conventional RAS1/RAS2/RAS3 notation,³⁴ the 12 orbitals are in RAS2 and consist of the $4s$ and five $3d$ orbitals of each Fe, and the 16 orbitals are in RAS3 and consist of five correlating $3d$ orbitals (denoted $3d'$) and three correlating $3p$ orbitals (denoted $3p'$) for each Fe atom; RAS1 is empty.

We also performed calculations on Fe, Fe^+ , and Fe^- atoms individually. The active spaces for Fe and Fe^+ were RAS(8,6;2,8) and RAS(7,6;2,8), respectively. The six orbitals in RAS2 are the valence $4s$ and five $3d$, and the eight orbitals in RAS3 are the five $3d'$ and three $3p'$ orbitals. The RASSCF(9,6;2,8) calculation did not converge for Fe^- ; additional balance was needed, and a $4s'$ orbital was added to RAS2. (The addition of a $4s'$ did not significantly affect the results for the other systems investigated (Fe, Fe^+ , Fe_2 , Fe_2^- , and Fe_2^+), and so it was not included.) The calculations on Fe, Fe^+ , and Fe^- used C_1 spatial symmetry. For the 5D ($4s^23d^6$), 6D ($4s^13d^6$), and 4F ($4s^23d^7$) states of Fe, Fe^+ , and Fe^- , a (SA) RASSCF (SA-RASSCF)⁴² was performed with equal weighting on each state, followed by multi-state (MS) RASPT2 (MS-RASPT2).⁴³ The number of states included was equal to the number of degenerate components. To compute the 5D - 5F splitting in Fe, a twelve-state SA-RASSCF was used because convergence of only the seven 5F higher-energy states was not feasible. The 5D and 5F states used for computing the splitting were from the twelve-state SA-RASSCF.

To further understand the EPR results of Ref. 17, we also performed calculations in which spin-orbit coupling was included. This was accomplished by the RAS-state-interaction-with-spin-orbit-coupling (RASSI-SO) method.⁴⁴ The diagonal elements of the RASSI-SO Hamiltonian were shifted by the MS-RASPT2 energies. The ZFS parameter, D , was extracted by mapping the eigenvalues of the RASSI-SO onto a model spin Hamiltonian,¹⁹

$$\hat{H}_{\text{mod}} = D\hat{S}_z. \quad (2)$$

Eight states were included in the RASSI-SO, namely the lowest-energy solutions for the 7A_g , $^7B_{1g}$, $^7B_{2g}$, $^7B_{3g}$, 9A_g , $^9B_{1g}$, $^9B_{2g}$, and $^9B_{3g}$ states. These states were chosen because they are of the same inversion symmetry as the predicted $^9\Sigma_g^-$ ground state (g and u states are not coupled through the SO term). The dependence on the number of states included in the RASSI-SO was investigated. Tests with 16 (two lowest-energy solutions of each of the above states) and 36 states (eight lowest-energy nonet states and the lowest-energy septet state) gave similar results.

To characterize the bonding, we computed the effective bond order (EBO), defined by⁴⁵

$$\text{EBO} = \frac{\eta_b - \eta_{\text{ab}}}{2}, \quad (3)$$

TABLE I. Computed properties of Fe atom as a function of active space.

	5D - 5F (eV) ^a	IP (eV) ^b
MS-CASPT2(8,6)	1.59	8.52
MS-CASPT2(8,11)	1.04	7.73
MS-CASPT2(8,14)	1.10	7.83
Expt.	0.87 ^c	7.90 ^d

^aFe(5F)-Fe(5D).^bFe+ (6D)-Fe(5D).^cNave *et al.*⁴⁶^dSugar and Corliss.⁴⁷

where η_b is the sum of occupation numbers of the bonding natural orbitals and η_{ab} is the sum of occupation numbers of the antibonding natural orbitals.

III. RESULTS

A. Exploratory work for choosing active space

The RAS(16,12;2,16) active space for Fe_2 was selected after a series of exploratory calculations. These calculations showed that the full-valence CAS(16,12) active space previously used in the literature is not sufficient. The dissociation energy that we computed with CASPT2(16,12) is 2.98 eV, which is in poor agreement with the experimental value of 1.15 eV.²² In addition we found that the small active spaces used previously can lead to potential energy curves that are not smooth functions of internuclear distance. Therefore the active space had to be increased. In order to study the requirements for a well-balanced active space, we studied the iron atom. We computed the 5D - 5F splitting and IP for Fe with the CAS(8,6), CAS(8,11), and CAS(8,14) active spaces as reported in Table I. The CAS(8,11) adds five correlating $3d'$ orbitals to the five valence $3d$ orbitals already present in the CAS(8,6) space, and the CAS(8,14) adds three $3p'$ orbitals to the CAS(8,11) calculation. The CAS(8,6) results reported in Table I further confirm that the CAS(16,12) active space for Fe_2 is insufficient. Since the CAS(8,11) for the Fe atom agrees well with experiment, a CAS(16,22) active space for Fe_2 would be desirable, but this is currently computationally prohibitive. However, a RAS(16,12;2,10) for Fe_2 , with the same orbital space as the CAS(16,22), is feasible. The RAS(16,12;2,10) active space was still not sufficient since the $3d'$ orbitals rotate out of the active space and are replaced by $3p'$ orbitals at internuclear distances near the equilibrium one. Thus, we enlarged the active space to also include $3p'$ orbitals, resulting in the RAS(16,12;2,16) (16 electrons in 28 orbitals in total) active space used in this work, where the notation is fully explained in Sec. II (Table II).

TABLE II. Number of CSFs for the $^9B_{1g}$ state^a of Fe_2 with various active spaces.

	CASSCF (16,12)	CASSCF (16,15)	CASSCF (16,22)	RASSCF ^b (16,12;2,16)
CSFs	64	71 788	10 ⁷	546 004

^aRecall that we use the D_{2h} point group; see Sec. II.^bSixteen electrons in 28 orbitals in total.

TABLE III. Relative energies (in eV) of three low-lying states of Fe₂ at 2.02 Å as compared to experimental and computational results.

	RASPT2 (16,12;2,16)	^a OPBE	NEVPT2 ^b (16,12)	NEVPT3 ^b (16,12)	CASPT2 ^c (16,12)	CASPT2 ^c (16,15)	MRCI+Q ^{Pd} (16,12)	Exp. ^e
⁹ Σ _g ⁻	0.00	0.00	0.00	0.00	0.00	0.00	0.00	0.00
⁷ Σ _g ⁻	0.58							0.53
⁷ Δ _u	0.64	-0.08	0.66	0.57	0.84	0.19	0.70	

^aCervantes-Salguero and Seminario.¹¹^bAngeli and Cimraglia.¹⁵^cBauschlicher and Ricca.²³^dHübner and Sauer.²⁴^eNegative ion PE experiment by Leopold *et al.*^{16,21}

B. Results for Fe₂

The total energies of the possible candidates for the ground state of Fe₂ were computed at the experimental bond distance, 2.02 Å, and a complete report of all states investigated in our calculations on Fe₂ is reported in supplementary material⁴⁸ in Tables S1 and S2 (tables numbered with an S are in the supplementary material). The three lowest-energy states are also reported in Table III, which shows that our calculations predict a ⁹Σ_g⁻ ground state for Fe₂. Table III compares our results for the relative energies of the low-lying states with those predicted by other recent computational studies and the negative ion PE experiment. First, we see that the OPBE exchange-correlation functional predicts the wrong ground state.¹¹ This is not entirely surprising because previous works that use the PBE correlation functional, namely PBEPBE, also predicted the ⁷Δ_u to be the ground state.⁴⁹ Our results agree well with the NEVPT results obtained with the smaller CAS(16,12). The ⁷Σ_g⁻ state is the first excited state observed in our calculations, and the energy difference from the ground state agrees well with the experimental negative ion PE result in the last column. Also in Table III, we compare our results to other computational studies. Bauschlicher and Ricca observed a decrease in the ⁹Σ_g⁻-⁷Δ_u splitting from 0.84 eV to 0.19 eV upon the inclusion of three 3*d* orbitals.²³ In comparing the same splitting in CASPT2(16,15) to RASPT2, we do not observe a further decrease from the CASPT2(16,12) value. It could be argued that the CAS(16,15) is an unbalanced active space due to the uneven treatment of the nearly degenerate 3*d* orbitals. Our work agrees well with the MRCI+Q^P calculation of Hübner and Sauer.²⁴ This seems to indicate that the electronic state splittings in Fe₂ do not require the 28-orbital active space in the reference wave function if the smaller space is well balanced.

Fe₂ does not have an orbitally degenerate ground state. To try to understand why the EPR experiment of Baumann *et al.* did not observe a signal for Fe₂, we computed the ZFS parameter, *D*, with the RASSI-SO method. We estimate it to be between 0 cm⁻¹ and 2 cm⁻¹, which is much less than the 8 cm⁻¹ upper limit given for their apparatus. The EPR experiment attempted to trap Fe₂ in a 4 K Ar matrix or a 4 K Kr matrix. The resonance Raman experiment by Moskovits and Di Lella isolated Fe₂ at 11 K in an Ar matrix,¹² so it seems likely that the experimental conditions should have been sufficient in the EPR study. Because Fe₂ appears to be trappable

and does not have a singlet ground state, an orbitally degenerate ground state, or a large ZFS, it is not clear to the present authors why the EPR signal was not detected.

The ground state of Fe₂ is dominated (73% weight) by the (4*s*σ_g)²(4*s*σ_u)¹(3*d*σ_g)²(3*d*σ_u)¹(3*d*π_u)⁴(3*d*π_g)²(3*d*δ_g)²(3*d*δ_u)² electronic configuration, which corresponds to a formal double bond. The effective bond order is 1.6, indicating a bond that is weaker than a double bond. Our calculated ground state potential energy curve for Fe₂ is shown in Figure 1. The potential energy curve in Figure 1 exhibits a barrier to dissociation because the ground adiabatic state has an avoided crossing. This is due to a crossing of two diabatic potentials; at large internuclear distances the wave function has the character of two ⁵*D* Fe atoms, which have the configuration 4*s*²3*d*⁶, whereas at small internuclear distances the wave function has the character a ⁵*D* Fe atom interacting with a ⁵*F* Fe atom, which has the configuration 4*s*¹3*d*⁷. We consider the adiabatic potential energy curve, consisting of the lowest-energy solution at all geometries, to try to understand a probable dissociation pathway of Fe₂. Total energies and the RASPT2 reference weights are reported in Table S7 in the supplementary material.⁴⁸ For further discussion of the diabatic potentials responsible for the potential in Figure 1, see Sec. III C.

The presence of a barrier raises an important issue concerning the experimental dissociation energy of Fe dimer. As

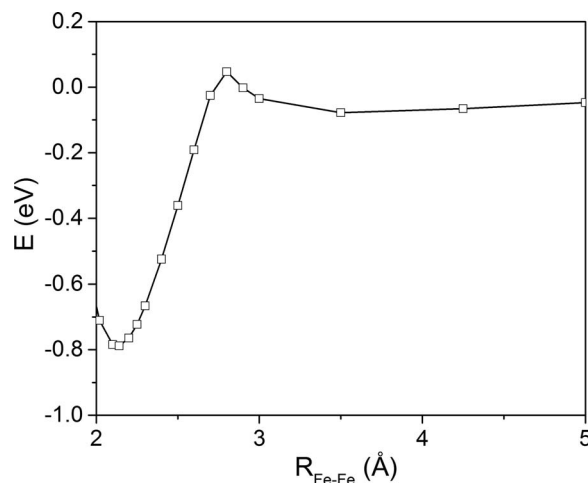


FIG. 1. Adiabatic ground state of Fe₂ computed by RASPT2(16,12;2,16)/ANO-RCC-VQZP. The energies are relative to the calculation on Fe₂ at 2.0 Å.

TABLE IV. Comparison of computed Fe_2 properties with those from experiment.

	R_e (Å)	ω_e (cm^{-1})	D_0 (eV)	EA (eV)	IP (eV)
RASPT2	2.13	325	0.77	0.38 ^a	6.04 ^a
Expt.	2.02 ^b	299.6 ^c	1.15 ^d	0.90 ^e	6.30 ^f

^aValue computed adiabatically.^bPurdum *et al.*¹⁴^cMoskovits and DiLella.¹²^dLoh *et al.*²²^eLeopold *et al.*^{16,21}^fRohlfing *et al.*⁶

reviewed in Sec. I, the dissociation energy of Fe_2 was determined by CID. A dissociation energy determined by CID may be too high if there is a barrier to dissociation like the one seen in Figure 1. However, Loh *et al.* did not measure the dissociation energy of Fe_2 directly. Instead, they measured it for Fe_2^+ and used Eq. (1) to compute it for Fe_2 . To investigate the accuracy of the experimentally measured D_0 , we therefore calculated the potential energy curve of Fe_2^+ to learn whether it has a barrier to dissociation; this will be discussed in Sec. III E.

Computed properties for Fe_2 are reported in Table IV. The IP of Fe_2 shows fairly good agreement with experiment (0.26 eV error), further corroborating our assignments for the ground states of Fe_2 and Fe_2^+ . See Sec. III E for further information on Fe_2^+ . The computed EA for Fe_2 has a rather large deviation (0.52 eV) from the experimental value (Table IV). To better understand the source of discrepancy between experiment and theory, we considered a single atom again, and the results are reported in Table V. Comparing Tables IV and V shows that the computed IP and EA of Fe are affected by similar discrepancies from the corresponding experimental values as the molecule (IP computed-measured discrepancy: 0.23 eV for Fe versus 0.26 eV for Fe_2 ; EA computed-measured discrepancy: 0.52 eV for both Fe and Fe_2). Such an error in the EA of Fe has already been documented³⁷ in a previous CASPT2 study. Roos *et al.*³⁷ concluded that the PT2 treatment causes large errors for transition metal atoms with an EA smaller than 0.5 eV.³⁷ See Sec. III D for further information on Fe_2^- . The 5D - 5F splitting in the atom reflects some of the error in D_0 of Fe_2 because a 5D to 5F transition must occur in one Fe atom to form the $^9\Sigma_g^-$ state of Fe_2 .

C. Electronic states contributing to the Fe_2 potential energy curve

In the absence of spin-orbit coupling, three different adiabatic states contribute to the ground-state potential energy

TABLE V. Comparison of computed Fe properties with those from experiment.

	5D - 5F (eV)	EA (eV)	IP (eV)
RASPT2	0.79 ^d	-0.37 ^c	7.67 ^f
Expt.	0.87 ^a	0.15 ^b	7.90 ^e

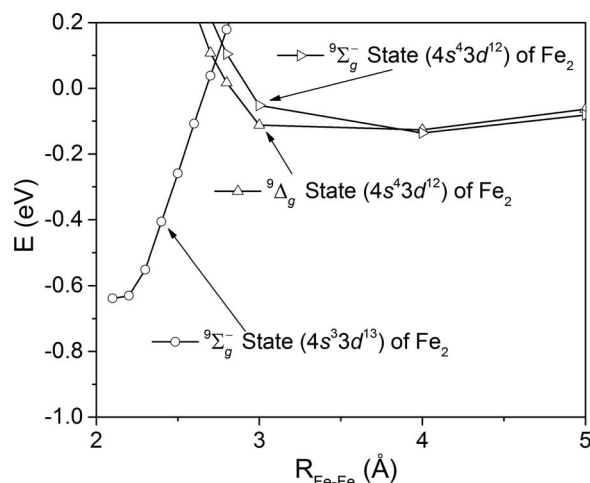
^aNave *et al.*⁴⁶^bLeopold and Lineberger.^{16,21}^cSugar and Corliss.⁴⁷^d $\text{Fe}(^5F) - \text{Fe}(^5D)$.^e $\text{Fe}(^5D) - \text{Fe}(^4F)$.^f $\text{Fe}^+(^6D) - \text{Fe}(^5D)$.

FIG. 2. The electronic states that contribute to the ground-state potential energy curve of Fe_2 that is reported in Figure 1. The calculations were performed at the MS(3)-RASPT2(16,12;2,16)/ANO-RCC-VTZP level of theory from a SA(5)-RASSCF(16,12;2,16) reference wave function. The $4s^3 3d^{13}$ and $4s^4 3d^{12}$ configurations were labeled with respect to the separated atoms $\text{Fe}^*(4s^1 3d^7) + \text{Fe}(4s^2 3d^6)$ and $\text{Fe}(4s^2 3d^6) + \text{Fe}(4s^2 3d^6)$, respectively.

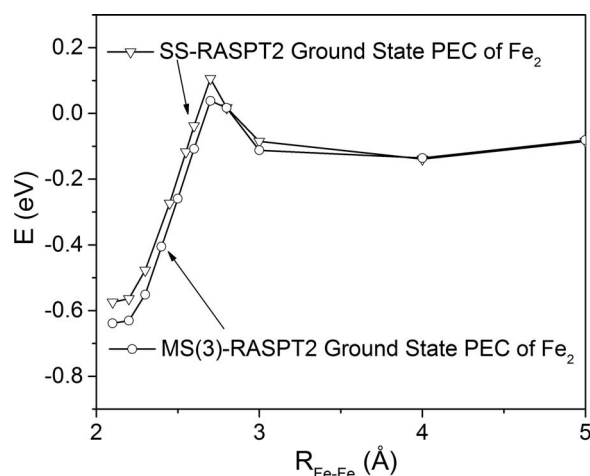


FIG. 3. The adiabatic ground-state potential energy curve of Fe_2 computed at two different levels of theory. The MS(3)-RASPT2(16,12;2,16)/ANO-RCC-VTZP calculation was computed with a SA(5)-RASSCF(16,12;2,16) reference wave function (the 3 states are the ones shown in Figure 2). The SS-RASPT2(16,12;2,16)/ANO-RCC-VTZP calculation was computed with a RASSCF(16,12;2,16) wave function.

TABLE VI. Relative energies (in eV) of four low-lying states of Fe_2^- at 2.10 Å are compared with previously reported theoretical results.

	RASPT2	CASPT2 ^a	MRCI ^b
$^8\Sigma_u^-$	0.00	0.00	0.0
$^8\Delta_u$	0.67		0.5
$^8\Pi_g$	0.71		0.5
$^8\Delta_{gu}$	0.91	-0.41	0.7

^aBauschlicher and Ricca.²³^bHübner and Sauer.²⁴

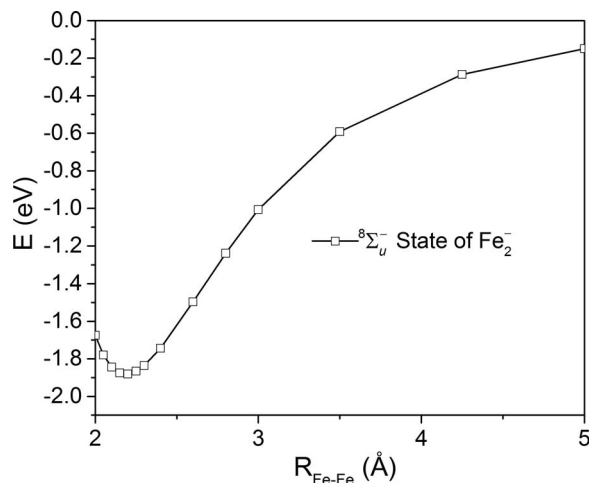


FIG. 4. Adiabatic ground state of Fe_2^- computed by RASPT2/ANO-RCC-VQZP. The energies are relative to the calculation on Fe_2^- at 20 Å.

curve of Fe_2 , as shown in Figure 2; that is, depending on the internuclear distance, three different adiabatic potentials take turns being lowest in energy. We first discovered this in exploratory calculations at the SA(5)-RASSCF(16,12;2,16)/ANO-RCC-VTZP level of theory. When dynamical correlation is included with MS(3)-RASPT2(16,12;2,16), we obtain the curves in Figure 2.

We observed that the SA(5)-RASSCF(16,12;2,16)/ANO-RCC-VTZP followed by MS(3)-RASPT2(16,12;2,16)/ANO-RCC-VTZP ground-state potential energy curve differs very little from a SS-RASPT2(16,12;2,16) ground-state potential energy curve as shown in Figure 3. The RASSCF(16,12;2,16) wave function was converged to the lowest-energy state seen in Figure 2, which very often did not correspond to the solution from an initial guess corresponding to the lowest-energy state at a nearby geometry. We recommend that future studies use state-averaged calculations as a tool for identifying the lowest-energy state along potential energy curves rather than using the variational solution without exploration of the orthogonal complement in configuration interaction space. Because of the results in Figure 3, we used SS-RASPT2 (which is a less expensive calculation) to study Fe_2 , Fe_2^+ , and Fe_2^- with the larger ANO-RCC-VQZP basis set.

D. Results for Fe_2^-

To further investigate the negative ion PE experiment result, we predicted the ground state of the iron dimer anion. The lowest-energy state in each irreducible representation of

TABLE VII. Comparison of computed Fe_2^- properties with those from experiment.

	R_e (Å)	ω_e (cm^{-1})	D_0 (eV)
RASPT2	2.19	288	1.86
Expt.	2.10 ^a	250 ± 20 ^a	1.90 ^b

^aLeopold *et al.*^{16,21}

^bLoh *et al.*²²

TABLE VIII. Relative energies (in eV) of four states of Fe_2^+ at 2.10 Å are compared with previously reported theoretical results. There are no experimental values available.

	RASPT2	CCSD(T) ^a	B3LYP ^b	BPW91 ^b
$^8\Sigma_u^-$	0.00	0.00	0.00	0.0
$^8\Delta_u$	0.46	-0.44	-1.06	-1.19
$^{10}\Sigma_g^-$	1.34	-0.95	0.32	0.72
$^{10}\Sigma_u^+$	2.75	-0.43	-1.48	1.14

^aIrigoras *et al.*⁵⁰

^bChiodo *et al.*⁵²

the D_{2h} point group with $S = 7/2$ spin symmetry was computed at the experimental geometry, 2.10 Å. A complete report of all states investigated in our calculations on Fe_2^- can be found in Tables S3 and S4 in the supplementary material.⁴⁸ The low-lying states are also in Table VI, which shows that the $^8\Sigma_u^-$ state is predicted to be the ground state in agreement with one of the two previously reported computations.²⁴

The ground state of Fe_2^- is dominated (71% weight) by the $(4s\sigma_g)^2(4s\sigma_u)^2(3d\sigma_g)^2(3d\sigma_u)^1(3d\pi_u)^4(3d\pi_g)^2(3d\delta_g)^2(3d\delta_u)^2$ configuration, which corresponds to a formal bond order of 3/2. The effective bond order⁴⁵ (EBO) is 1.1, indicating a bond that is closer to a single bond. This electronic configuration is in agreement with the interpretation of their experiment by Leopold *et al.*¹⁶ Our calculated adiabatic ground state potential energy curve for Fe_2^- is reported in Figure 4. The total energies and RASPT2 reference weights are reported in Table S8 in the supplementary material.⁴⁸ For further validation that the $^8\Sigma_u^-$ is the ground state, R_e , ω_e , and D_0 of Fe_2^- are compared to experimental results in Table VII. These results are in good agreement. The bond length difference between Fe_2 and Fe_2^- (0.06 Å) shows good agreement with the bond length difference obtained by Leopold *et al.* (0.08 Å).^{16,21}

E. Results for Fe_2^+

There are few experimental measurements on Fe_2^+ and previous computational studies predicted a different

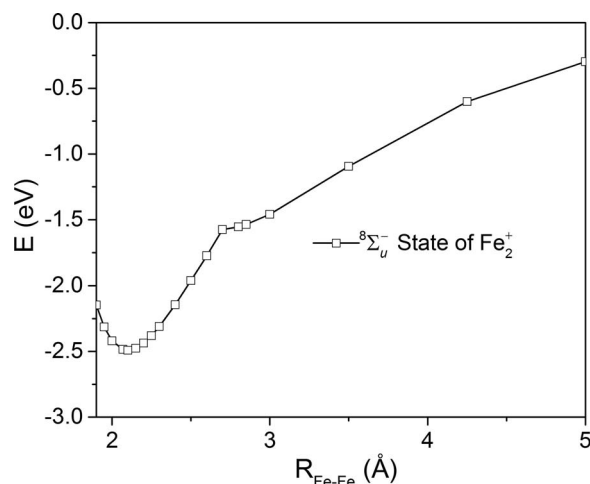


FIG. 5. Adiabatic ground state potential energy curve of Fe_2^+ computed by RASPT2/ANO-RCC-VQZP. The energies are relative to the calculation on Fe_2^+ at 20 Å.

TABLE IX. Computed spectroscopic constants for Fe_2^+ .

	R_e (Å)	ω_e (cm^{-1})	D_0 (eV)
RASPT2	2.10	345	2.47
Expt.			2.72 ^a

^aLoh *et al.*²²

electronic ground state.^{50–52} Both octet and decet states were investigated at the RASPT2/ANO-RCC-VQZP level of theory. These calculations were performed at the equilibrium bond distance of the $^8\Sigma_u^-$ state, 2.10 Å. A complete report of all states investigated in our calculations on Fe_2^+ is presented in Tables S5 and S6 in the supplementary material.⁴⁸ The low-lying states are in Table VIII, which reveals large discrepancies among the methods.

The ground state of Fe_2^+ is dominated (71% weight) by the $(4s\sigma_g)^2(3d\sigma_g)^2(3d\sigma_u)^1(3d\pi_u)^4(3d\pi_g)^2(3d\delta_g)^2(3d\delta_u)^2$ electronic configuration, which corresponds to a formal bond order of 5/2. The EBO is 2.0, indicating a bond that is much closer to a double bond. The adiabatic ground state potential energy curve for Fe_2^+ is reported in Figure 5. The total energies and RASPT2 reference weights are reported in Table S9 in the supplementary material.⁴⁸

The potential energy curve in Figure 5 exhibits a small bump at 2.7 Å, but there is no barrier to dissociation. At an internuclear distance larger than 2.7 Å, a 5D Fe atom interacts attractively with a 6D Fe^+ , which has the configuration $4s^13d^6$, whereas at distances smaller than 2.7 Å an electron of Fe^+ is promoted from the $4s^13d^6$ configuration (6D) to a $3d^7$ configuration (4F). We can draw two important conclusions from Figure 5. The first concerns the ground-state electronic configuration of Fe_2^+ . Because the ground state $4s^23d^{13}$ configuration of Fe_2^+ can be formed from a one-electron detachment of the ground state $4s^33d^{13}$ configuration of Fe_2 , the IP reported in the photoionization study of Rohlffing *et al.* corresponds to the IP of ground state Fe_2 .⁶ The second important conclusion is related to the barrier observed in Figure 1 for Fe_2 . Because there is no barrier to dissociation in Figure 5, the experimentally reported D_0 for Fe_2^+ is not thrown in doubt.

The computed equilibrium bond distance, harmonic frequency, and dissociation energy for the ground state of the Fe_2^+ are reported in Table IX. To our knowledge only the experimental dissociation energy is available for comparison from the literature.

IV. CONCLUSIONS

A computational investigation of the iron dimer has been reported, and direct comparison with available experimental data has been presented. We predicted the ground states of Fe_2 , Fe_2^- , and Fe_2^+ to be $^9\Sigma_g^-$, $^8\Sigma_u^-$, and $^8\Sigma_u^-$, respectively. We cannot explain why the transition between M_S components was not observed in a previous EPR study of Fe_2 ;¹⁷ however, we show that it was not due to an orbitally degenerate ground state or large zero-field splitting. We recommend that the EPR experiment should be revisited.

We found that the previously used CAS(16,12) active space for Fe_2 ^{15,23,24} is not able to correctly predict the IP and D_0 of Fe_2 . By using a much larger active space, within the RAS formalism, RAS(16,12;2,16) (16 electrons in 28 orbitals), we make significantly more accurate predictions. This shows the value of the RASSCF and RASPT2 methods, which allow one to address problems that are too large to be treated by CASSCF or CASPT2. Moreover, the active space employed in these calculations, 16 electrons in 28 orbitals, represents a record in terms of size. Conventional CASPT2 calculations can be performed with at most 16 electrons in 16 orbitals. We were able to overcome this limit by using the RASSCF and RASPT2 formalism instead.

We report the first multireference study of Fe_2^+ . We find that although the ground-state potential energy curve of Fe_2 has a barrier, that of Fe_2^+ does not. With the exception of the EA of Fe_2 , our results for Fe_2^- are in good agreement with photoelectron spectroscopy.

ACKNOWLEDGMENTS

We thank Dongxia Ma and Rémi Maurice for help with the calculations and Doreen Leopold for useful discussions of iron dimer. This work was supported by the (U.S.) Department of Energy (DOE), Office of Basic Energy Sciences, under SciDAC Grant No. DE-SC0008666.

- S. C. Richtsmeier, E. K. Parks, K. Liu, L. G. Pobo, and S. J. Riley, *J. Chem. Phys.* **82**, 3659 (1985).
- E. K. Parks, G. Nieman, L. G. Pobo, and S. J. Riley, *J. Chem. Phys.* **88**, 6260 (1988).
- B. Weiller, P. Bechthold, E. K. Parks, L. G. Pobo, and S. J. Riley, *J. Chem. Phys.* **91**, 4714 (1989).
- J. B. Griffin and P. B. Armentrout, *J. Chem. Phys.* **107**, 5345 (1997).
- L. Tan, F. Liu, and P. B. Armentrout, *J. Chem. Phys.* **124**, 084302 (2006).
- E. A. Rohlffing, D. M. Cox, A. Kaldor, and K. H. Johnson, *J. Chem. Phys.* **81**, 3846 (1984).
- E. K. Parks, B. H. Weiller, P. S. Bechthold, W. F. Hoffman, G. C. Nieman, L. G. Pobo, and S. J. Riley, *J. Chem. Phys.* **88**, 1622 (1988).
- S. Chrétien and D. R. Salahub, *Phys. Rev. B* **66**, 155425 (2002).
- G. L. Gutsev and C. W. Bauschlicher, Jr., *J. Phys. Chem. A* **107**, 7013 (2003).
- H. J. Kulik, M. Cococcioni, D. A. Scherlis, and N. Marzari, *Phys. Rev. Lett.* **97**, 103001 (2006).
- K. Cervantes-Salguero and J. M. Seminario, *J. Mol. Model.* **18**, 4043 (2012).
- M. Moskovits and D. P. DiLella, *J. Chem. Phys.* **73**, 4917 (1980).
- T. C. De Vore, A. Ewing, H. F. Franzen, and V. Calder, *Chem. Phys. Lett.* **35**, 78 (1975).
- H. Purdum, P. A. Montano, G. K. Shenoy, and T. Morrison, *Phys. Rev. B* **25**, 4412 (1982).
- C. Angeli and R. Cimiriaglia, *Mol. Phys.* **109**, 1503 (2011).
- D. G. Leopold, J. Almlöf, W. C. Lineberger, and P. R. Taylor, *J. Chem. Phys.* **88**, 3780 (1988).
- C. A. Baumann, R. J. Van Zee, and W. Weltner, Jr., *J. Phys. Chem.* **88**, 1815 (1984).
- R. J. Van Zee, C. M. Brown, K. J. Zeringue, and W. Weltner, Jr., *Acc. Chem. Res.* **13**, 237 (1980).
- A. Abragam and B. Bleaney, *Electron Paramagnetic Resonance of Transition Ions* (Clarendon Press, Oxford, 1970), Vol. 1.
- W. Weltner, Jr., *Magnetic Atoms and Molecules* (Van Nostrand Reinhold Company Inc., 1983).
- D. G. Leopold and W. C. Lineberger, *J. Chem. Phys.* **85**, 51 (1986).
- S. Loh, L. Lian, D. A. Hales, and P. B. Armentrout, *J. Phys. Chem.* **92**, 4009 (1988).
- C. W. Bauschlicher, Jr. and A. Ricca, *Mol. Phys.* **101**, 93 (2003).
- O. Hübner and J. Sauer, *Chem. Phys. Lett.* **358**, 442 (2002).

- ²⁵B. O. Roos, P. R. Taylor, and P. E. M. Siegbahn, *Chem. Phys.* **48**, 157 (1980).
- ²⁶H.-J. Werner and P. J. Knowles, *J. Chem. Phys.* **89**, 5803 (1988).
- ²⁷S. R. Langhoff and E. R. Davidson, *Int. J. Quant. Chem.* **8**, 61 (1974).
- ²⁸K. Andersson, P.-Å. Malmqvist, B. O. Roos, A. J. Sadlej, and K. Wolinski, *J. Phys. Chem.* **94**, 5483 (1990).
- ²⁹K. Andersson and B. O. Roos, *Chem. Phys. Lett.* **191**, 507 (1992).
- ³⁰J. Pople, R. Seeger, and R. Krishnan, *Int. J. Quant. Chem.* **12**, 149 (1977).
- ³¹C. Angeli, M. Pastore, and R. Cimiraglia, *Theor. Chem. Acc.* **117**, 743 (2007).
- ³²N. C. Handy and A. Cohen, *J. Mol. Phys.* **99**, 403 (2001).
- ³³J. P. Perdew, K. Burke, and M. Ernzerhof, *Phys. Rev. Lett.* **77**, 3865 (1996).
- ³⁴J. Olsen, B. O. Roos, P. Jørgensen, and H. J. A. Jensen, *J. Chem. Phys.* **89**, 2185 (1988).
- ³⁵P.-Å. Malmqvist, K. Pierloot, A. R. M. Shahi, C. J. Cramer, and L. Gagliardi, *J. Chem. Phys.* **128**, 204109 (2008).
- ³⁶F. Aquilante, L. DeVico, N. Ferré, G. Ghigo, P.-Å. Malmqvist, P. Neogrády, T. B. Pedersen, M. Pitoňák, M. Reiher, B. O. Roos, L. Serrano-Andrés, M. Urban, V. Veryazov, and R. Lindh, *J. Comput. Chem.* **31**, 224 (2010).
- ³⁷B. O. Roos, R. Lindh, P.-Å. Malmqvist, V. Veryazov, and P. O. Widmark, *J. Phys. Chem. A* **109**, 6575 (2005).
- ³⁸B. A. Hess, *Phys. Rev. A* **33**, 3742 (1986).
- ³⁹M. F. Guest and V. R. Saunders, *Mol. Phys.* **28**, 819 (1974).
- ⁴⁰N. Forsberg and P.-Å. Malmqvist, *Chem. Phys. Lett.* **274**, 196 (1997).
- ⁴¹G. Ghigo, B. O. Roos, and P.-Å. Malmqvist, *Chem. Phys. Lett.* **396**, 142 (2004).
- ⁴²H.-J. Werner and W. Meyer, *J. Chem. Phys.* **74**, 5794 (1981).
- ⁴³J. Finley, P.-Å. Malmqvist, B. O. Roos, and L. Serrano-Andrés, *Chem. Phys. Lett.* **288**, 299 (1998).
- ⁴⁴P.-Å. Malmqvist, *Int. J. Quantum Chem.* **30**, 479 (1986); P.-Å. Malmqvist and B. O. Roos, *Chem. Phys. Lett.* **155**, 189 (1989); P.-Å. Malmqvist, B. O. Roos, and B. Schimmelpfennig, *ibid.* **357**, 230 (2002); P.-Å. Malmqvist and B. O. Roos, *Phys. Chem. Chem. Phys.* **6**, 2919 (2004).
- ⁴⁵B. O. Roos, A. C. Borin, and L. Gagliardi, *Angew. Chem., Int. Ed.* **46**, 1469 (2007).
- ⁴⁶G. Nave, S. Johansson, R. C. M. Learner, A. P. Thorne, and J. W. Brault, *Astrophys. J. Suppl. Ser.* **94**, 221 (1994).
- ⁴⁷J. Sugar and C. Corliss, *J. Phys. Chem. Ref. Data* **14**(Suppl. 2), 1 (1985).
- ⁴⁸See supplementary material at <http://dx.doi.org/10.1063/1.4901718> where we report the total energies, relative energies, CASPT2 reference weights, and electronic character of all investigated electronic states of Fe₂, Fe₂⁺, and Fe₂⁻. In addition, we provide total energies and reference weights corresponding to the PECs in Figs. 1, 4, and 5.
- ⁴⁹A. Sorkin, M. A. Iron, and D. G. Truhlar, *J. Chem. Theory Comput.* **4**, 307 (2008).
- ⁵⁰A. Irigoras, M. d. C. Michelini, E. Sicilia, N. Russo, J. M. Mercero, and J. M. Ugalde, *Chem. Phys. Lett.* **376**, 310 (2003).
- ⁵¹G. L. Gutsev and C. W. Bauschlicher, Jr., *J. Phys. Chem. A* **107**, 4755 (2003).
- ⁵²S. Chiodo, I. Rivalta, M. d. C. Michelini, N. Russo, E. Sicilia, and J. M. Ugalde, *J. Phys. Chem. A* **110**, 12501 (2006).